
On the Role of Entropy-based Loss for Learning Causal Structures with Continuous Optimization

Ruichu Cai¹, Weilin Chen¹, Jie Qiao^{1*}, Zhifeng Hao^{1,2}

¹ School of Computer Science, Guangdong University of Technology, China

² School of Mathematics and Big Data, Foshan University, China

cairuichu@gdut.edu.cn, chenweilin.chn@gmail.com, qiaojie.chn@gmail.com, zfhao@gdut.edu.cn

Abstract

Causal discovery from observational data is an important but challenging task in many scientific fields. Recently, NOTEARS [Zheng et al., 2018] formulates the causal structure learning problem as a continuous optimization problem using least-square loss with an acyclicity constraint. Though the least-square loss function is well justified under the standard Gaussian noise assumption, it is limited if the assumption does not hold. In this work, we theoretically show that the violation of the Gaussian noise assumption will hinder the causal direction identification, making the causal orientation fully determined by the causal strength as well as the variances of noises in the linear case and the noises of strong non-Gaussianity in the nonlinear case. Consequently, we propose a more general entropy-based loss that is theoretically consistent with the likelihood score under any noise distribution. We run extensive empirical evaluations on both synthetic data and real-world data to validate the effectiveness of the proposed method and show that our method achieves the best in Structure Hamming Distance, False Discovery Rate, and True Positive Rate matrices.

1 Introduction

Learning causal structure from observational data has become an important topic in many scientific fields, such as economics [Ghysels et al., 2016], biology [Grosse-Wentrup et al., 2016], and social science [Cai et al., 2016]. Due to the expensive cost or the ethic of randomized experiments, the task of causal discovery from purely observational data has been drawn much attention.

Many approaches have been proposed for learning causal structure. Traditionally, by utilizing the conditional independence property among observed variables, the constraint-based approaches have been proposed, e.g., PC algorithm [Spirtes et al., 2000], but only identify the underlying directed acyclic graph (DAG) up to Markov equivalence class [Andersson et al., 1997]. Alternatively, by introducing a certain class of Structure Causal Model (SCM), and further assuming the causal mechanism that the noise and the hypothetical cause are independent, the functional-based causal models have been proposed, e.g., the Linear Non-Gaussian Acyclic Model (LiNGAM) [Shimizu et al., 2006], the Additive Noise Model (ANM) [Hoyer et al., 2008], and the Post-Nonlinear causal Model (PNL) [Zhang and Hyvärinen, 2009]. However, due to the intractable search space superexponential in graph nodes, learning DAGs using functional-based causal models is challenging.

Recently, NOTEARS [Zheng et al., 2018], under the additive noise model assumption, formulates the causal structure learning problem as a continuous optimization problem using least-square loss with a continuous DAG constraint. Such a technique has been extensively developed and applied to learning linear or nonlinear causal structures. Yu et al. [2019] introduces a variational autoencoder framework

*Corresponding author.

for modeling the generative process of a causal structure equipped with evidence lower bound with a Gaussian prior of noise which is implemented by least-square loss. Ng et al. [2019b] and Zheng et al. [2020] extend a linear causal model into a nonlinear causal model using neural networks but still rely on the least-square loss for reconstruction.

However, our analysis shows that using least-square loss as the score function will hinder the causal direction identification. In a linear system, such loss will be highly influenced by the causal strengths and the noise variances leading to a bias estimation comparing with the likelihood score. In a more general nonlinear system, the causal direction will be incorrectly identified if noise distribution has strong non-Gaussianity property.

In this paper, we show that the entropy-based loss is consistent with the likelihood score under the additive noise model using any noise distribution, and thus we advocate using the entropy-based loss instead of least-square loss. Overall, our contributions are as follows:

1. In Section 4, we study the limitations of least-square loss and provide theoretical bounds that least-square loss will fail to identify the causal direction in a linear and nonlinear system, respectively.
2. In Section 5, we build a connection between the entropy-based loss and the log-likelihood score, and further provide the theory for its validity.
3. In Section 6, we run extensive experiments over linear and nonlinear systems by using both synthetic data and real-world data and show our method performs more effectively and stably.

2 Related Works

Related to least-square loss: Blöbaum et al. [2018, 2019] address the problem of inferring the causal relation between two variables using least-square loss under the modularity property, i.e., the independence between the function and the distribution of cause. Peters and Bühlmann [2014] prove the full identifiability of the linear Gaussian structural equation in case that all noise variables have the same variance.

Related to NOTEARS: Yu et al. [2019] proposes an alternative characterization of acyclicity and utilizes a generative model to learn the nonlinear causal structure. Ng et al. [2019b] utilizes a graph autoencoder framework to extend the linear SCM to nonlinear SCM. Ng et al. [2019a] extends to nonlinearity by putting the weighted matrix on the first layer of MLP. Lachapelle et al. [2019] expresses weighted matrix by neural network paths to deal with the nonlinear case. Zheng et al. [2020] proposes a more general acyclicity constraint based on partial derivatives to support nonlinear models.

3 Preliminary

3.1 Structure Causal Model

Causal discovery problems can be formalized by a Structure Causal Model (SCM) [Didelez and Pigeot, 2001]. Given a set of random variables $X = \{X_1, X_2, \dots, X_d\}$ and the corresponding noises $N = \{N_1, N_2, \dots, N_d\}$, SCM between X_i and its direct parents $X_{pa_{\mathcal{G}}(i)}$ with respect to a DAG \mathcal{G} is defined as follows:

$$X_i = f_i(X_{pa_{\mathcal{G}}(i)}, N_i), \quad (1)$$

where f_i could be a linear or nonlinear function. Following the previous works [Zheng et al., 2018], we consider the additive noise model, i.e., $X_i = f_i(X_{pa_{\mathcal{G}}(i)}) + N_i$, and assume the causal sufficiency holds.

3.2 NOTEARS

Zheng et al. [2018] proposed a continuous optimization for learning causal structure, using least-square loss with an acyclicity constraint. Given a set of observational data $\{x_1^{(i)}, \dots, x_d^{(i)}\}_{i=1}^m$ which is sampled from a joint distribution $p(X)$, we assume that the joint distribution is Markov with

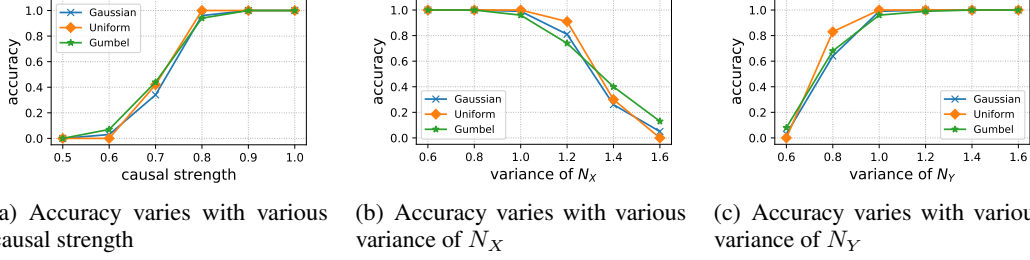


Figure 1: Control experiments of accuracy with respect to different conditions in linear system. At each experiments, we will control one of the parameters while fix others. The default parameters are set as $\alpha = 0.5$, $\sigma_{N_X} = 2$, and $\sigma_{N_Y} = 1$. And the controlled parameters will varies form $\alpha = [0.5, 1]$, $\sigma_{N_X} = [0.6, 1.6]$, $\sigma_{N_Y} = [0.6, 1.6]$.

respect to a ground truth DAG \mathcal{G} and can be factorized as $p(X) = \prod_{i=1}^d p(X_i | X_{pa_{\mathcal{G}}(i)})$. Then the corresponding design matrix is $\mathbf{X} \in \mathbb{R}^{m \times d}$. In particular, the directed graph in a linear SCM can be encoded by a weighted adjacency matrix $W \in \mathbb{R}^{d \times d}$, i.e., $X = W^{\top} X + N$. Zheng et al. [2018] shows that W represents a DAG if and only if $\text{tr}(e^{W \circ W}) - d = 0$ holds, where \circ denotes the Hadamard product. Then, NOTEARS formulates the causal structure learning problem as the following continuous optimization problem:

$$\arg \min_{W \in \mathbb{R}^{d \times d}} \frac{1}{2m} \|\mathbf{X} - \mathbf{X}W\|_F^2 + \lambda \|W\|_1 \quad \text{subject to} \quad \text{tr}(e^{W \circ W}) - d = 0, \quad (2)$$

where $\frac{1}{2m} \|\mathbf{X} - \mathbf{X}W\|_F^2$ is the least-square loss and is equal, up to constant, to the log-likelihood score of a linear Gaussian DAG with equal noise variances, and $\|W\|_1$ denotes the ℓ_1 penalty term on the causal structure.

4 Limitations of Least-Square Loss

This section discusses why methods based on least-square loss fail to discover the underlying causal structure, and we theoretically show the conditions that they fail in both linear and nonlinear cases.

Without loss of generality, we analyze the causal pair of two variables, and assume that:

$$\begin{aligned} X &= N_X, \\ Y &= \begin{cases} \alpha X + N_Y & \text{Linear} \\ f(X) + N_Y & \text{Nonlinear} \end{cases} \end{aligned} \quad (3)$$

where the variance $\text{Var}(N_X) = \sigma_{N_X}^2$, $\text{Var}(N_Y) = \sigma_{N_Y}^2$, $N_X \perp\!\!\!\perp N_Y$, and f is a nonlinear function.

To see the limitations of least-square loss, we take the two variables as an example. We run NOTEARS 100 times using the least-square loss with 400 samples per experiment in linear Gaussian, Uniform, and Gumbel data. As shown in Figure 1, the accuracy is highly controlled by the causal strength as well as the noise variance. We see that using the least-square loss, NOTEARS could fail even under the non-Gaussian distribution that is notably identifiable [Shimizu et al., 2006]. The reason is the mismatch between the truth distribution and the standard Gaussian distribution implied by the least-square loss. In addition, due to the non-identifiability of the linear Gaussian causal model, the causal direction can still be controlled by the causal strength and the noise variance.

Next, we will formally analyze the condition that least-square loss fails to identify the causal direction in the linear and nonlinear cases.

4.1 Linear Case

In the linear case, let $X \rightarrow Y$ denotes the causal direction from cause X to effect Y , and let $Y \rightarrow X$ denote the anti-causal direction. Let σ_X^2 denote the variance of variable X . Let $\beta_{Y|X}$ be the linear

regression coefficient obtained from regressing Y on X , and let $\sigma_{Y|X}^2 = \text{Var}(Y - \beta_{Y|X} \cdot X)$ be the variance of the residual of regressing Y on X .

Then, for the causal direction, we have:

$$\sigma_{X|\phi}^2 = \sigma_{N_X}^2, \quad \beta_{Y|X} = \frac{\alpha\sigma_X^2}{\sigma_X^2} = \alpha, \quad \sigma_{Y|X}^2 = \sigma_{N_Y}^2. \quad (4)$$

For the reverse direction, we have:

$$\begin{aligned} \sigma_{Y|\phi}^2 &= \alpha^2 \sigma_{N_X}^2 + \sigma_{N_Y}^2, \quad \beta_{X|Y} = \frac{\alpha\sigma_{N_X}^2}{\sigma_{Y|\phi}^2} = \frac{\alpha\sigma_{N_X}^2}{\alpha^2\sigma_{N_X}^2 + \sigma_{N_Y}^2}, \\ \sigma_{X|Y}^2 &= \text{Var}(X - \beta_{X|Y}Y) = \frac{\sigma_{N_X}^2\sigma_{N_Y}^2}{\alpha^2\sigma_{N_X}^2 + \sigma_{N_Y}^2}. \end{aligned} \quad (5)$$

Note that NOTEARS will prefer the direction that has a smaller least-square loss. Thus, we are interested to see in what condition NOTEARS will fail, i.e., the least-square loss satisfying $LS_{X \rightarrow Y} > LS_{Y \rightarrow X}$. By using the above derivation, we can show such a condition in the following theorem.

Theorem 1. *Let $X \rightarrow Y$ be the causal direction following the data generation mechanism $X = N_X, Y = \alpha X + N_Y$. The least-square loss will fail to identify the correct causal direction if the causal strength α , the noise variances $\sigma_{N_X}^2$ and $\sigma_{N_Y}^2$ satisfy the following inequality:*

$$\alpha^2 < 1 - \frac{\sigma_{N_Y}^2}{\sigma_{N_X}^2}. \quad (6)$$

Proof. Note that the least-square loss in the additive noise model is equivalent to the summation of estimated noise variance. Thus, using the Eq. (4), the least-square loss in the direction of $X \rightarrow Y$ is given as follows:

$$LS_{X \rightarrow Y} = \mathbb{E}[(X - 0)^2] + \mathbb{E}[(Y - \beta_{Y|X} \cdot X)^2] = \sigma_{N_X}^2 + \sigma_{N_Y}^2, \quad (7)$$

where $\beta_{Y|X}$ is the coefficient obtained from linear regression. Similarly, using Eq. (5), we obtain

$$LS_{Y \rightarrow X} = \mathbb{E}[(X - \beta_{X|Y} \cdot Y)^2] + \mathbb{E}[(Y - 0)^2] = \frac{\sigma_{N_Y}^2\sigma_{N_X}^2}{\alpha^2\sigma_{N_X}^2 + \sigma_{N_Y}^2} + \alpha^2\sigma_{N_X}^2 + \sigma_{N_Y}^2. \quad (8)$$

Using Eq. (7) and (8), we consider the condition that the loss in causal direction is larger than the loss in the reverse direction, i.e., $LS_{X \rightarrow Y} > LS_{Y \rightarrow X}$, and we obtain (6). The details of derivation are given in Appendix A. \square

Theorem 1 indicates that, under the linear additive noise model assumption, the least-square loss could fail to identify the correct causal direction unless the inequality (6) does not hold. It is also interesting to see that if all noises follow the standard Gaussian distribution, we have $\sigma_{N_X}^2 = \sigma_{N_Y}^2$, then the causal direction can still be correctly identified because the inequality $\alpha^2 < 0$ must not hold. However, it is unrealistic that all noises follow the same standard Gaussian distribution in the real world. And a simple standardization that is usually used for preprocessing will invalidate the assumption. In addition, Theorem 1 also explains the experiments in Figure 1 that why the change of causal strength or the noise variance will change the causal orientation.

Therefore, we conclude that the least-square loss is not a suitable score for learning linear causal structure.

4.2 Nonlinear Case

In the nonlinear case, we study SCM between $X \rightarrow Y$ with the nonlinear additive form $Y = f(X) + N_Y$. To show the limitation of least-square loss in a nonlinear case, we aim to show that using the least-square loss can be viewed as minimizing the mutual information between the noise and cause variables but with bias such that the independence measure will be not reliable, leading to identify the wrong direction. To do so, we first show that maximizing likelihood is equivalent to

minimizing the mutual information between the cause and the noise variables (Lemma 1). Then, we further show that maximizing the likelihood under the standard Gaussian noise assumption is equivalent to minimizing the least-square loss (Lemma 2). Combing with Lemma 1 and Lemma 2, we conclude that using least-square loss, the mutual information will be biased (Lemma 3). Finally, by considering the bias in mutual information, we provide the condition that least-square loss fails in Theorem 2.

To be clear, let \hat{f} denote the function of regressing Y on X , and \hat{g} denote the function of regressing X on Y . Keep in mind that N_X and N_Y are the noise variables. To avoid ambiguity, we denote that: $\hat{N}_Y := Y - \hat{f}(X)$ and $\hat{N}_X := X - \hat{g}(Y)$. Let $J_{X \rightarrow Y}$ denote the Jacobian matrix of the transformation from $(X, N_Y)^T$ to $(X, Y)^T$, i.e., $J_{X \rightarrow Y} = \begin{pmatrix} \frac{\partial X}{\partial X} & \frac{\partial X}{\partial N_Y} \\ \frac{\partial Y}{\partial X} & \frac{\partial Y}{\partial N_Y} \end{pmatrix}$, and let $J_{Y \rightarrow X}$ denote the Jacobian matrix of the transformation from $(Y, \hat{N}_X)^T$ to $(Y, X)^T$.

Lemma 1 (Theorem 2 in Zhang et al. [2015]). *Given samples $\{x^{(i)}, y^{(i)}\}_{i=1}^m$, and the causal model $Y = f(X, N_Y; \theta)$ with any parameters θ and the estimated residual \hat{N}_Y , the log-likelihood $l_{X \rightarrow Y}(\theta)$ and the mutual information between X and \hat{N}_Y are related in the following way:*

$$I(X, \hat{N}_Y; \theta) = \frac{1}{m} \sum_{i=1}^m \log p(X = x^{(i)}, Y = y^{(i)}) - \frac{1}{m} l_{X \rightarrow Y}(\theta), \quad (9)$$

where

$$l_{X \rightarrow Y}(\theta) = \sum_{i=1}^m \log p(X = x^{(i)}) + \sum_{i=1}^m \log p(N_Y = \hat{n}_Y^{(i)}; \theta) - \sum_{i=1}^m \log \left| \frac{\partial f}{\partial N_Y} \Big|_{N_Y = \hat{n}_Y^{(i)}} \right|. \quad (10)$$

Lemma 1 builds a connection between the log-likelihood and the mutual information. In the following Lemma, we further build the connection between log-likelihood and the least-square loss.

Lemma 2. *For the additive noise model $Y = f(X) + N_Y$, maximizing the log-likelihood $l_{X \rightarrow Y}(\theta)$ with the standard Gaussian noise assumption:*

$$l_{X \rightarrow Y}(\theta) = \sum_{i=1}^m \log \left(\frac{1}{\sqrt{2\pi}} \exp \left(-\frac{(x^{(i)} - 0)^2}{2} \right) \right) + \sum_{i=1}^m \log \left(\frac{1}{\sqrt{2\pi}} \exp \left(-\frac{(y^{(i)} - \hat{f}(x^{(i)}; \theta))^2}{2} \right) \right) - \sum_{i=1}^m \log \left| \frac{\partial f}{\partial N_Y} \Big|_{N_Y = \hat{n}_Y^{(i)}} \right|.$$

is equivalent to minimizing the least-square loss $LS_{X \rightarrow Y}$:

$$LS_{X \rightarrow Y} = \mathbb{E} \left[(X - 0)^2 \right] + \mathbb{E} \left[(Y - \hat{f}(X))^2 \right].$$

Based on Lemma 1 and Lemma 2, one can straightforward develop the following Lemma that using the least-square loss will introduce the standard Gaussian distribution in the mutual information.

Lemma 3. *For the additive noise model, minimizing the least-square loss is equivalent to minimizing the mutual information under the standard Gaussian noise assumption with the following form:*

$$I_q(X, \hat{N}_Y; \theta) = \frac{1}{m} \left(\sum_{i=1}^m \log p(X = x^{(i)}, Y = y^{(i)}) - \sum_{i=1}^m \log q(X = x^{(i)}) - \sum_{i=1}^m \log q(N_Y = \hat{n}_Y^{(i)}; \theta) \right), \\ = \mathbb{E}_{x, y \sim p(x, y)} [\log p(X = x, Y = y) - \log q(X = x) - \log q(N_Y = \hat{n}_Y; \theta)]. \quad (11)$$

where q is the density function of standard Gaussian distribution.

Based on Lemma 3, in the following theorem, we show that in what condition the least-square loss will fail.

Theorem 2. *Let $X \rightarrow Y$ be the causal direction following the data generation mechanism $Y = f(X) + N_Y$. The causal direction is non-identifiable using least-square loss if the following inequality holds:*

$$-\int p(X) \log q(X) - \int p(N_Y) \log q(N_Y) > -\int p(Y) \log q(Y) - \int p(\hat{N}_X) \log q(\hat{N}_X), \quad (12)$$

where q is the density function of standard Gaussian distribution.

Proof. Without loss of generality, we assume the identifiability condition of the additive noise model holds. Then, we have $I(X, N_Y) < I(Y, \hat{N}_X)$. However, based on Lemma 3, using the least-square loss, the mutual information becomes:

$$\begin{aligned} I_q(X, N_Y) &= - \int p(X) \log q(X) - \int p(N_Y) \log q(N_Y) + \int p(X, Y) \log p(X, Y), \\ I_q(Y, \hat{N}_X) &= - \int p(Y) \log q(Y) - \int p(\hat{N}_X) \log q(\hat{N}_X) + \int p(X, Y) \log p(X, Y), \end{aligned} \quad (13)$$

where $q \sim N(0, I)$. In this cases, the inequality $I_q(X, N_Y) < I_q(Y, \hat{N}_X)$ is not necessary holds. In fact, by solving the inequality $I_q(X, N_Y) > I_q(Y, \hat{N}_X)$ using (13), we obtain (12), which is the condition that least-square fails. \square

Theorem 2 shows that if inequality (12) holds, the least-square loss could fail especially when Kullback-Leibler divergence between distribution $p(X)$ or $p(N_Y)$ and the standard Gaussian distribution is large.

For example, let $Y = \text{sigmoid}(X) + N_Y$ where $X \sim \text{Uniform}(-C, C)$ and $N_Y \sim \text{Uniform}(-1, 1)$. In this case, we can simply increase C such that $-\int p(X) \log q(X)$ will tend to infinity while Y and \hat{N}_X are bounded due to the sigmoid function, such that the right hand side in (12) are also bound, and hence the inequality must hold.

Therefore, it is necessary to use the correct distribution setting $q = p$ to obtain the correct result, which inspires a way that uses the entropy-based loss instead.

5 Structure Learning Using Entropy-based Loss

As discussed in Section 4, using least-square loss, which is equivalent to assuming the distribution of all noise terms is standard Gaussian distribution, will result in the incorrect causal identification. The reason for these errors is the mismatch of the truth distribution and the assumed standard Gaussian distribution.

Instead of using the square operator in least-square loss, we can replace it with the entropy such that:

$$\min \sum_{i=1}^d H(N_i) + \lambda \|W\|_1 \quad \text{subject to} \quad \text{tr}(e^{W \circ W}) - d = 0, \quad (14)$$

where $H(N_i) = -\int p(N_i) \log p(N_i)$ denotes the entropy of variable N_i .

To explain why we use entropy-based loss, we first show that the entropy-based loss is consistent with the log-likelihood score under the additive noise model (see Theorem 3). Based on Theorem 3, by utilizing identifiability results in terms of likelihood, it is easy to show that the entropy-based loss is also identifiable.

Theorem 3. *In additive noise model, the entropy-based score has a consistency with the log-likelihood score when the sample sizes $m \rightarrow \infty$, that is*

$$\frac{1}{m} \sum_{j=1}^m \sum_{i=1}^d \log p(x_i^{(j)} | x_{pa_G(i)}^{(j)}) = - \sum_{i=1}^d H(N_i). \quad (15)$$

Theorem 3 indicates that, under the additive noise model, the entropy-based loss is consistent with the log-likelihood score, while Peters et al. [2014] had proven that under the ANM model, the log-likelihood is able to distinguish the causal direction under a mild assumption. Hence, the entropy-based loss has the same property, which is illustrated in the following corollary:

Corollary 1. *For each pair of additive noise model $Y = f(X) + N_Y$, if $v''(Y - f(X))f'(X) \neq 0$ and the following condition holds:*

$$\xi''' = \xi'' \left(-\frac{v''' f'}{v''} + \frac{f''}{f'} \right) - 2v'' f'' f' + v' f''' + \frac{v' v''' f'' f'}{v''} - \frac{v'(f'')^2}{f'}, \quad (16)$$

where $v := \log p(N_Y)$, $\xi := \log p(X)$, then using the entropy-based loss each pair of additive model is identifiable and the following inequality holds:

$$H(X) + H(\hat{N}_Y) < H(Y) + H(\hat{N}_X). \quad (17)$$

Corollary 1 illustrates the validity of the entropy-based loss under the additive noise model, which is based on the consistency with the likelihood score, indicating that by comparing the entropy of residuals between causal and anti-causal direction, we can identify the cause and effect variables in most cases.

6 Experiments

To investigate the effectiveness of the entropy loss, we compare it with baseline algorithms on both synthetic data and real-world data. The synthetic data are generated from linear non-Gaussian data and nonlinear additive noise data, respectively. The following algorithms that use the least-square loss for data reconstruction are taken as the baseline: NOTEARS [Zheng et al., 2018], DAG-GNN [Yu et al., 2019], NOTEARS-MLP [Zheng et al., 2020]. We reuse the parameter settings for those baseline algorithms in their original papers and codes.

For the differential entropy estimator, it turn out that the method proposed by Hyvärinen [1998] is well suit for this problem. in which the entropy can be estimated using following method:

$$H(X) \approx H(\nu) - \left[k_1 (E\{\bar{G}_1(X)\})^2 + k_2 (E\{\bar{G}_2(X)\} - E\{\bar{G}_2(\nu)\})^2 \right], \quad (18)$$

where $k_1 = 36/(8\sqrt{3}-9)$, $k_2 = 24/(16\sqrt{3}-27)$, $\bar{G}_1(X) = X \exp(-X^2/2)$, $\bar{G}_2(X) = \exp(-X^2/2)$, $\bar{G}_2(\nu) = \sqrt{1/2}$, and $H(\nu) = \frac{1}{2}(1 + \log(2\pi))$.

Our implementation, denoted by **ours** (linear) and **ours-MLP** (nonlinear), is based on the codes of NOTEARS [Zheng et al., 2018] and NOTEARS-MLP [Zheng et al., 2020], respectively. Following the previous works, the numerical optimize algorithms L-BFGS [Byrd et al., 1995] is used for optimization, and we will prune the edges after training with a small threshold $\omega = 0.3$ to rule out cycle-inducing edges.

In linear non-Gaussian case, the data are generated according to the following linear structure equations, $X_i = \sum_{j \in pa_G(i)} \beta_{ij} X_j + N_j$ with random causal strength $\beta_{ij} \sim \text{Uniform}(-0.4, -0.8) \cup \text{Uniform}(0.4, 0.8)$ and the noise $N_j \sim \sigma_{N_j} * \text{Uniform}(-\sqrt{3}, \sqrt{3})$ or $N_j \sim \sigma_{N_j} * \text{Gumbel}(0, \frac{\sqrt{6}}{\pi})$ with random standard deviation $\sigma_{N_j} \sim \text{Uniform}(0.5, 1.0)$. In nonlinear case, the data are generated according to the following nonlinear SCM: $X_i = \tanh(\sum_{j \in pa_G(i)} \beta_{1,ij} X_j) + \cos(\sum_{j \in pa_G(i)} \beta_{2,ij} X_j) + \sin(\sum_{j \in pa_G(i)} \beta_{3,ij} X_j) + N_j$ with random causal strength $\beta_{k,ij} \sim \text{Uniform}(0.5, 2.0)$ for $k = 1, 2, 3$ and the noise $N_j \sim \sigma_{N_j} * \text{Uniform}(-\sqrt{3}, \sqrt{3})$ with random standard deviation $\sigma_{N_j} \sim \text{Uniform}(0.5, 1.0)$.

Following previous works, Structural Hamming Distance (SHD), False Discovery Rate (FDR), and True Positive Rate (TPR) are recorded as the evaluation metrics for all algorithms.

6.1 Synthetic Structures

In this section, we design a series of controlled experiments with respect to the sample sizes and the number of variables on the synthetic random causal structures. At each experiment, we will control one of the parameters while fixing others. The range of the above controlled parameters are as follows: the number of samples={200, 400, **600**, 800, 1000} and the number of variables= {5, 10, **15**, 20, 25} with in-degree=2 where the default setting is marked as bold. All experiments will run at least ten times.

6.1.1 Linear Case

In this part, we perform linear experiments on the synthetic linear non-Gaussian data. Here, we test our method on Uniform and the Gumbel distribution, respectively. Each algorithm runs 30 times for all experiments.

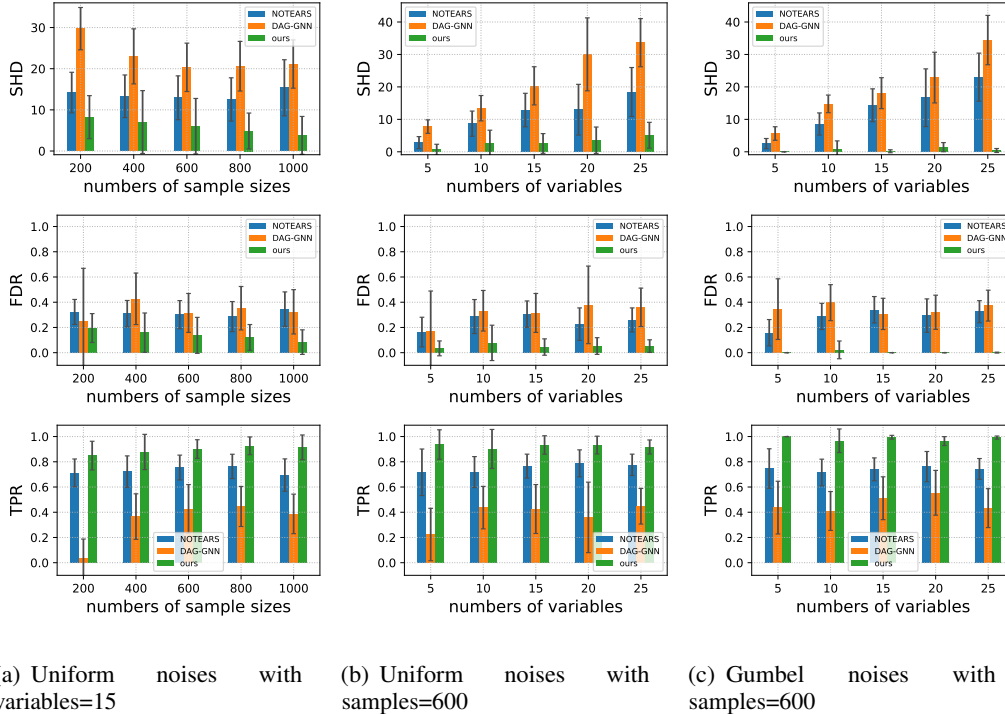


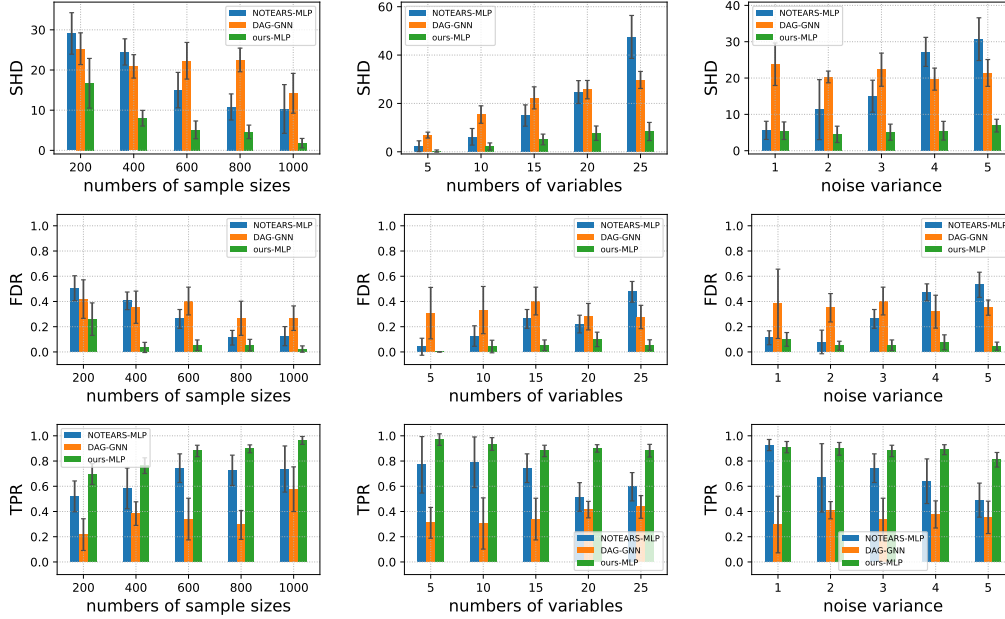
Figure 2: Structure recovery in linear data in terms of SHD, FDR and TPR to the true graph: in Figure 2(a), the noises are Uniform, the number of variables and edges are 15 and 30; in Figure 2(b), the noises are Uniform, and the sample sizes are 600; in Figure 2(c), the noises are Gumbel, and the sample sizes are 600.

As shown in Figure 2, our method outperforms all baseline methods on the three controlled experiments. Moreover, by using the entropy-based method, we have the least deviation error. It is also interesting to see the significant difference between ours and the NOTEARS, which verifies that the algorithm could learn the reverse causal direction using least-square loss. In detail, in Figure 2(a), as the sample size increase, all methods has the better performance, and we can see that when the sample size is small, we still outperform the other methods, which shows the robustness of our method. In Figure 2(b) and 2(b), in general, the performance decrease as the number of variables increases, but compared with the baseline methods, our method decreases slowly. In addition, we can see that under different distributions, our method has similar performance within experimental errors, which verifies the Theorem 1.

6.1.2 Nonlinear Case

In this part, we test our entropy-based loss in nonlinear data. To further verify the Theorem 3 we generate the nonlinear data using Uniform distribution with different variances. That is, the higher the variance, the more non-Gaussianity. In the controlled experiments we further test our method on different noise variance={1, 2, 3, 4, 5}. Each algorithm will run at least ten times.

The results are given in Figure 3. Overall, our method generally outperforms the baseline methods showing the robustness of our method in variable-varying and variance-varying cases. In detail, in Figure 3(a), we notice that comparing with the linear data, all methods require more data to acquire a decent performance, but our method still outperforms the baseline methods. For our method, 600 is a decent choice for the sample sizes. In figure 3(b), with the growing number of variables, the performance of NOTEARS-MLP decreases rapidly while our method remains stable. The reason is that as the number of variables grows, the edges increase simultaneously, and the incorrectly identified edges will also increase. In Figure 3(b), we can see that our method is not sensitive to the noise variances while the performance of other methods decreases rapidly as the variances grow. The reason is that the variance controls the noise non-Gaussianity making it far from the standard



(a) Uniform noises with variables=15

(b) Uniform noises with samples=600

(c) Uniform noises with variables=15

Figure 3: Structure recovery in nonlinear data in terms of SHD, FDR and TPR to the true graph: in figure 3(a), the noises are uniform with variance=3.0 and the number of variables and edges are 15 and 30; in Figure 3(b), the noises are Uniform with variance=3.0 and the number of sample sizes is 600; in Figure 3(c), the noises are Uniform, the number of sample sizes is 600, and the number of variables and edges are 15 and 30.

Gaussian. Therefore, the entropy-based loss is stable and identifiable under any distribution while other methods will lose its identifiability.

6.2 Real-World Data

Following previous works, we use the real-world data set provided by Sachs et al. [2005]. This data set contains 7466 groups of continuous expression levels of 20 measured molecules in human immune system cells. The consensus network, accepted by the biological community, is represented by a Bayesian network with 11 variables and 20 edges. Compared with NOTEARS that predicts 16 edges with an SHD of 22, **ours** predicts 19 edges with an SHD of 21, which shows the effectiveness of our method with higher recall and precision. Compared with NOTEARS-MLP predicting 13 edges with an SHD of 16, and DAG-GNN predicting 18 edges with an SHD of 19, **ours-MLP** has a similar result predicting 13 edges with an SHD of 16.

7 Conclusion

In this work, we re-examine the least-square loss for learning causal structures in causal discovery and advocate to use a more general entropy-based loss as the objective function. Our analysis shows that the least-square loss is problematic to learn the underlying causal structure if the standard Gaussian noise assumption does not hold. On the contrary, the entropy-based loss is consistent with the log-likelihood score, which is robust and effective for learning causal structures. Our experimental results verify the proposed theoretical results and show the effectiveness of the proposed entropy-based loss. A clear next step is to generalize the theory and algorithms to a more general causal mechanism.

References

- Steen A Andersson, David Madigan, Michael D Perlman, et al. A characterization of markov equivalence classes for acyclic digraphs. *Annals of statistics*, 25(2):505–541, 1997.
- Patrick Blöbaum, Dominik Janzing, Takashi Washio, Shohei Shimizu, and Bernhard Schölkopf. Cause-effect inference by comparing regression errors. In *International Conference on Artificial Intelligence and Statistics*, pages 900–909. PMLR, 2018.
- Patrick Blöbaum, Dominik Janzing, Takashi Washio, Shohei Shimizu, and Bernhard Schölkopf. Analysis of cause-effect inference by comparing regression errors. *PeerJ Computer Science*, 5: e169, 2019.
- Richard H Byrd, Peihuang Lu, Jorge Nocedal, and Ciyu Zhu. A limited memory algorithm for bound constrained optimization. *SIAM Journal on scientific computing*, 16(5):1190–1208, 1995.
- Ruichu Cai, Zhenjie Zhang, Zhifeng Hao, and Marianne Winslett. Understanding social causalities behind human action sequences. *IEEE transactions on neural networks and learning systems*, 28(8):1801–1813, 2016.
- Vanessa Didelez and Iris Pigeot. Judea pearl: Causality: Models, reasoning, and inference. *Politische Vierteljahresschrift*, 42(2):313–315, 2001.
- Eric Ghysels, Jonathan B Hill, and Kaiji Motegi. Testing for granger causality with mixed frequency data. *Journal of Econometrics*, 192(1):207–230, 2016.
- Moritz Grosse-Wentrup, Dominik Janzing, Markus Siegel, and Bernhard Schölkopf. Identification of causal relations in neuroimaging data with latent confounders: An instrumental variable approach. *NeuroImage*, 125:825–833, 2016.
- Patrik Hoyer, Dominik Janzing, Joris M Mooij, Jonas Peters, and Bernhard Schölkopf. Nonlinear causal discovery with additive noise models. *Advances in neural information processing systems*, 21:689–696, 2008.
- Aapo Hyvärinen. New approximations of differential entropy for independent component analysis and projection pursuit. In *Proceedings of the 1997 Conference on Advances in Neural Information Processing Systems 10*, NIPS ’97, page 273–279, Cambridge, MA, USA, 1998. MIT Press. ISBN 0262100762.
- Sébastien Lachapelle, Philippe Brouillard, Tristan Deleu, and Simon Lacoste-Julien. Gradient-based neural dag learning. *arXiv preprint arXiv:1906.02226*, 2019.
- Ignavier Ng, Zhuangyan Fang, Shengyu Zhu, Zhitang Chen, and Jun Wang. Masked gradient-based causal structure learning. *arXiv preprint arXiv:1910.08527*, 2019a.
- Ignavier Ng, Shengyu Zhu, Zhitang Chen, and Zhuangyan Fang. A graph autoencoder approach to causal structure learning. *arXiv preprint arXiv:1911.07420*, 2019b.
- Jonas Peters and Peter Bühlmann. Identifiability of gaussian structural equation models with equal error variances. *Biometrika*, 101(1):219–228, 2014.
- Jonas Peters, Joris M. Mooij, Dominik Janzing, and Bernhard Schölkopf. Causal discovery with continuous additive noise models. *Journal of Machine Learning Research*, 15(58):2009–2053, 2014. URL <http://jmlr.org/papers/v15/peters14a.html>.
- Karen Sachs, Omar Perez, Dana Pe’er, Douglas A Lauffenburger, and Garry P Nolan. Causal protein-signaling networks derived from multiparameter single-cell data. *Science*, 308(5721):523–529, 2005.
- Shohei Shimizu, Patrik O Hoyer, Aapo Hyvärinen, Antti Kerminen, and Michael Jordan. A linear non-gaussian acyclic model for causal discovery. *Journal of Machine Learning Research*, 7(10), 2006.
- Peter Spirtes, Clark N Glymour, Richard Scheines, and David Heckerman. *Causation, prediction, and search*. MIT press, 2000.

Yue Yu, Jie Chen, Tian Gao, and Mo Yu. Dag-gnn: Dag structure learning with graph neural networks. In *International Conference on Machine Learning*, pages 7154–7163. PMLR, 2019.

Kun Zhang and Aapo Hyvärinen. On the identifiability of the post-nonlinear causal model. In Jeff A. Bilmes and Andrew Y. Ng, editors, *UAI 2009, Proceedings of the Twenty-Fifth Conference on Uncertainty in Artificial Intelligence, Montreal, QC, Canada, June 18-21, 2009*, pages 647–655. AUAI Press, 2009.

Kun Zhang, Zhikun Wang, Jiji Zhang, and Bernhard Schölkopf. On estimation of functional causal models: general results and application to the post-nonlinear causal model. *ACM Transactions on Intelligent Systems and Technology (TIST)*, 7(2):1–22, 2015.

Xun Zheng, Bryon Aragam, Pradeep K Ravikumar, and Eric P Xing. Dags with no tears: Continuous optimization for structure learning. *Advances in Neural Information Processing Systems*, 31: 9472–9483, 2018.

Xun Zheng, Chen Dan, Bryon Aragam, Pradeep Ravikumar, and Eric Xing. Learning sparse nonparametric dags. In *International Conference on Artificial Intelligence and Statistics*, pages 3414–3425. PMLR, 2020.

Supplementary Material

A Proof of Theorem 1

Theorem 1. *Let $X \rightarrow Y$ be the causal direction following the data generation mechanism $X = N_X, Y = \alpha X + N_Y$. The least-square loss will fail to identify the correct causal direction if the causal strength α , the noise variances $\sigma_{N_X}^2$ and $\sigma_{N_Y}^2$ satisfy the following inequality:*

$$\alpha^2 < 1 - \frac{\sigma_{N_Y}^2}{\sigma_{N_X}^2}. \quad (\text{A.1})$$

Proof. Then, for the causal direction, we have:

$$\sigma_{X|\phi}^2 = \sigma_{N_X}^2, \quad \beta_{Y|X} = \frac{\alpha\sigma_X^2}{\sigma_X^2} = \alpha, \quad \sigma_{Y|X}^2 = \sigma_{N_Y}^2. \quad (\text{A.2})$$

For the anti-causal direction, we have

$$\begin{aligned} \sigma_{Y|\phi}^2 &= \alpha^2\sigma_{N_X}^2 + \sigma_{N_Y}^2, \quad \beta_{X|Y} = \frac{\alpha\sigma_{N_X}^2}{\sigma_{Y|\phi}^2} = \frac{\alpha\sigma_{N_X}^2}{\alpha^2\sigma_{N_X}^2 + \sigma_{N_Y}^2} \\ \sigma_{X|Y}^2 &= \text{Var}(X - \beta_{X|Y}Y) = \frac{\sigma_{N_X}^2\sigma_{N_Y}^2}{\alpha^2\sigma_{N_X}^2 + \sigma_{N_Y}^2}. \end{aligned} \quad (\text{A.3})$$

Note that the least-square loss in the additive noise model is equivalent to the summation of estimated noise variance. Thus, using the Eq. (A.2), the least-square loss in the direction of $X \rightarrow Y$ is given as follows:

$$LS_{X \rightarrow Y} = \mathbb{E}[(X - 0)^2] + \mathbb{E}[(Y - \beta_{Y|X} \cdot X)^2] = \sigma_{N_X}^2 + \sigma_{N_Y}^2, \quad (\text{A.4})$$

where $\beta_{Y|X}$ is the coefficient obtained from linear regression. Similarly, using Eq. (A.3), we obtain

$$LS_{Y \rightarrow X} = \mathbb{E}[(X - \beta_{X|Y} \cdot Y)^2] + \mathbb{E}[(Y - 0)^2] = \frac{\sigma_{N_Y}^2\sigma_{N_X}^2}{\alpha^2\sigma_{N_X}^2 + \sigma_{N_Y}^2} + \alpha^2\sigma_{N_X}^2 + \sigma_{N_Y}^2. \quad (\text{A.5})$$

Using Eq. (A.4) and (A.5), we consider the condition that the loss in causal direction is larger than the loss in the reverse direction, i.e., $LS_{X \rightarrow Y} > LS_{Y \rightarrow X}$, and we have the following inequality:

$$\begin{aligned}
\sigma_{N_X}^2 + \sigma_{N_Y}^2 &> \frac{\sigma_{N_Y}^2 \sigma_{N_X}^2}{\alpha^2 \sigma_{N_X}^2 + \sigma_{N_Y}^2} + \alpha^2 \sigma_{N_X}^2 + \sigma_{N_Y}^2 \\
\sigma_{N_X}^2 &> \left(\frac{\sigma_{N_Y}^2}{\alpha^2 \sigma_{N_X}^2 + \sigma_{N_Y}^2} + \alpha^2 \right) \sigma_{N_X}^2 \\
\alpha^2 &< 1 - \frac{\sigma_{N_Y}^2}{\alpha^2 \sigma_{N_X}^2 + \sigma_{N_Y}^2} \\
\alpha^2 &< \frac{\alpha^2 \sigma_{N_X}^2 + \sigma_{N_Y}^2 - \sigma_{N_Y}^2}{\alpha^2 \sigma_{N_X}^2 + \sigma_{N_Y}^2} \\
\alpha^2 &< \frac{\alpha^2}{\alpha^2 + \frac{\sigma_{N_Y}^2}{\sigma_{N_X}^2}} \\
\alpha^2 &< 1 - \frac{\sigma_{N_Y}^2}{\sigma_{N_X}^2}.
\end{aligned} \tag{A.6}$$

□

B Proof of Lemma 2

Lemma 1 (Theorem 2 in Zhang et al. [2015]). *Given samples $\{x^{(i)}, y^{(i)}\}_{i=1}^m$, and the causal model $Y = f(X, N_Y; \theta)$ with any parameters θ and the estimated residual \hat{N}_Y , the log-likelihood $l_{X \rightarrow Y}(\theta)$ and the mutual information between X and \hat{N}_Y are related in the following way:*

$$I(X, \hat{N}_Y; \theta) = \frac{1}{m} \sum_{i=1}^m \log p(X = x^{(i)}, Y = y^{(i)}) - \frac{1}{m} l_{X \rightarrow Y}(\theta), \tag{B.1}$$

where

$$l_{X \rightarrow Y}(\theta) = \sum_{i=1}^m \log p(X = x^{(i)}) + \sum_{i=1}^m \log p(N_Y = \hat{n}_Y^{(i)}; \theta) - \sum_{i=1}^m \log \left| \frac{\partial f}{\partial N_Y} \Big|_{N_Y = \hat{n}_Y^{(i)}} \right|. \tag{B.2}$$

Lemma 1 builds a connection between the log-likelihood and the mutual information. In the following Lemma, we further build the connection between log-likelihood and the least-square loss.

Lemma 2. *For the additive noise model $Y = f(X) + N_Y$, maximizing the log-likelihood $l_{X \rightarrow Y}(\theta)$ with the standard Gaussian noise assumption is equivalent to minimizing the least-square loss.*

Proof. Based on Lemma 1, the log-likelihood under the standard Gaussian distribution has the following form:

$$\begin{aligned}
l_{X \rightarrow Y}(\theta) &= \sum_{i=1}^m \log \left(\frac{1}{\sqrt{2\pi}} \exp \left(-\frac{(x^{(i)} - 0)^2}{2} \right) \right) + \sum_{i=1}^m \log \left(\frac{1}{\sqrt{2\pi}} \exp \left(-\frac{(y^{(i)} - \hat{f}(x^{(i)}; \theta))^2}{2} \right) \right) \\
&\quad - \sum_{i=1}^m \log \left| \frac{\partial f}{\partial N_Y} \Big|_{N_Y = \hat{n}_Y^{(i)}} \right|.
\end{aligned} \tag{B.3}$$

Note that, under the additive noise model, we have $\frac{\partial f}{\partial N_Y} = 1$, and thus last term in (B.3) will be vanish. Then, log-likelihood can be rewritten as follows:

$$l_{X \rightarrow Y}(\theta) = -\frac{1}{2} \sum_{i=1}^m \left[(x^{(i)} - 0)^2 + ((y^{(i)} - \hat{f}(x^{(i)}; \theta))^2) \right] + const. \tag{B.4}$$

Comparing with the least-square loss $LS_{X \rightarrow Y}$ that used in NOTEARS:

$$LS_{X \rightarrow Y} = \mathbb{E}[(X - 0)^2] + \mathbb{E}[(Y - \hat{f}(X))^2], \quad (\text{B.5})$$

we can see that maximizing the log-likelihood with standard Gaussian noise assumption is equivalent to minimizing the least-square loss. \square

C Proof of Lemma 3

Lemma 3. *For the additive noise model, minimizing the least-square loss is equivalent to minimizing the mutual information under the standard Gaussian noise assumption with the following form:*

$$\begin{aligned} I_q(X, \hat{N}_Y; \theta) &= \frac{1}{m} \left(\sum_{i=1}^m \log p(X = x^{(i)}, Y = y^{(i)}) - \sum_{i=1}^m \log q(X = x^{(i)}) - \sum_{i=1}^m \log q(N_Y = \hat{n}_Y^{(i)}; \theta) \right), \\ &= \mathbb{E}_{x, y \sim p(x, y)} [\log p(X = x, Y = y) - \log q(X = x) - \log q(N_Y = \hat{n}_Y; \theta)]. \end{aligned} \quad (\text{C.1})$$

where q is the density function of standard Gaussian distribution.

Proof. Based on Lemma 2, as Eq. (B.3) shown, using the least-square loss, the distribution in the log-likelihood will become Gaussian. Then, by substituting (B.3) into (B.1) we obtain (C.1) which is the mutual information under the standard Gaussian noise assumption. \square

D Proof of Theorem 3

Theorem 3. *In additive noise model, the entropy-based score has a consistency with the log-likelihood score when the sample sizes $m \rightarrow \infty$, that is*

$$\frac{1}{m} \sum_{j=1}^m \sum_{i=1}^d \log p(x_i^{(j)} | x_{pa_G(i)}^{(j)}) = - \sum_{i=1}^d H(N_i). \quad (\text{D.1})$$

Proof. Based on Lemma 1 we generalize the log-likelihood from two variables case to the multivariate case as follows:

$$\begin{aligned} \frac{1}{m} \sum_{j=1}^m \sum_{i=1}^d \log p(x_i^{(j)} | x_{pa_G(i)}^{(j)}) &= \frac{1}{m} \sum_{j=1}^m \sum_{i=1}^d \log p(N_i = \hat{n}_i^{(j)}) - \frac{1}{m} \sum_{j=1}^m \sum_{i=1}^d \log \left| \frac{\partial f_i}{\partial N_i} \Big|_{N_i = \hat{n}_i^{(j)}} \right| \\ &= \frac{1}{m} \sum_{j=1}^m \sum_{i=1}^d \log p(N_i = \hat{n}_i^{(j)}) = \sum_{i=1}^d -H(N_i). \end{aligned} \quad (\text{D.2})$$

The second equality is based on the property of the additive noise model in which $\frac{\partial f_i}{\partial N_i} = 1$. Then, as $m \rightarrow \infty$, we obtain the last equality. \square

E Proof of Corollary 1

Lemma 4 (Theorem 1 in Hoyer et al. [2008]). *For the additive noise model $Y = f(X) + N_Y$, there is a forward model of the form $p(X, Y) = p(Y - f(X))p(X)$. If there is a backward model of the same form $p(X, Y) = p(X - f(Y))p(Y)$, then for all X, Y with the three time differentiable f and $v''(Y - f(X))f'(X) \neq 0$, the following equality holds:*

$$\xi''' = \xi'' \left(-\frac{v''' f'}{v''} + \frac{f''}{f'} \right) - 2v'' f'' f' + v' f''' + \frac{v' v''' f'' f'}{v''} - \frac{v'(f'')^2}{f'}, \quad (\text{E.1})$$

where $v := \log p(N_Y)$, $\xi := \log p(X)$.

Lemma 4 guarantees that the asymmetry of independence only vanishes under strictly conditions. In most cases, such asymmetry exists and the ANM can be identified. Based on Lemma 4, we prove the asymmetry of entropy also exists for most cases.

Corollary 1. For each pair of additive noise model $Y = f(X) + N_Y$, if $v''(Y - f(X))f'(X) \neq 0$ and the following condition holds:

$$\xi''' = \xi'' \left(-\frac{v'''}{v''} \frac{f'}{f''} + \frac{f''}{f'} \right) - 2v'' f'' f' + v' f''' + \frac{v' v'' f'' f'}{v''} - \frac{v'(f'')^2}{f'}, \quad (\text{E.2})$$

where $v := \log p(N_Y)$, $\xi := \log p(X)$, then using the entropy-based loss each pair of additive model is identifiable and has the form $H(X) + H(\hat{N}_Y) < H(Y) + H(\hat{N}_X)$.

Proof. To be clear, let \hat{f} denote the function of regressing Y on X with a residual \hat{N}_Y , and let \hat{g} denote the function of regressing X on Y with a residual \hat{N}_X .

To prove corollary 1, we will compare the mutual information between hypothetical cause and the regression residual in causal and anti-causal direction. Assuming the backward model does not exist based on Lemma 4, the noise and the hypothetical cause is independent, i.e., $N_i \perp\!\!\!\perp X_{\text{pa}_{\mathcal{G}(i)}}$ in the causal direction, but not vice versa. Such a property can be represented by mutual information form as follows:

$$\begin{aligned} I(X, \hat{N}_Y) &< I(Y, \hat{N}_X) \\ \int p(X, \hat{N}_Y) \log \frac{p(X, \hat{N}_Y)}{p(X)p(\hat{N}_Y)} &< \int p(X, \hat{N}_Y) \log \frac{p(Y, \hat{N}_X)}{p(Y)p(\hat{N}_X)} \\ -\mathbb{E} \log p(X) - \mathbb{E} \log p(\hat{N}_Y) + \mathbb{E} \log p(X, \hat{N}_Y) &< -\mathbb{E} \log p(Y) - \mathbb{E} \log p(\hat{N}_X) + \mathbb{E} \log p(Y, \hat{N}_X) \\ H(X) + H(\hat{N}_Y) + \mathbb{E} \log p(X, \hat{N}_Y) &< H(Y) + H(\hat{N}_X) + \mathbb{E} \log p(Y, \hat{N}_X) \end{aligned} \quad (\text{E.3})$$

In fact, $p(X, \hat{N}_Y)$ and $p(Y, \hat{N}_X)$ can be transformed to $p(X, Y)$, and then be eliminated in both sides. We also denote X' and Y' for conveniently and clearly expressing the transformations as follows:

$$\text{causal direction: } \begin{cases} X' = X, \\ \hat{N}_Y = Y - \hat{f}(X). \end{cases} \quad \text{anti-causal direction: } \begin{cases} Y' = Y, \\ \hat{N}_X = X - \hat{g}(Y). \end{cases} \quad (\text{E.4})$$

Then, the distribution transformations from $(X, Y)^T$ to $(X', \hat{N}_Y)^T$ and $(X, Y)^T$ to $(Y', \hat{N}_X)^T$ are as follows:

$$p(X, Y) = p(X', \hat{N}_Y) |\det(J_{X \rightarrow Y})| \quad p(X, Y) = p(Y', \hat{N}_X) |\det(J_{Y \rightarrow X})|$$

and

$$\begin{aligned} |\det(J_{X \rightarrow Y})| &= \left| \det \begin{pmatrix} \frac{\partial X'}{\partial X} & \frac{\partial X'}{\partial Y} \\ \frac{\partial \hat{N}_Y}{\partial X} & \frac{\partial \hat{N}_Y}{\partial Y} \end{pmatrix} \right| = \left| \det \begin{pmatrix} \frac{\partial X}{\partial(Y - \hat{f}(X))} & \frac{\partial X}{\partial(Y - \hat{f}(X))} \\ \frac{\partial X}{\partial X} & \frac{\partial X}{\partial Y} \end{pmatrix} \right| = \left| \det \begin{pmatrix} 1 & 0 \\ -\frac{\partial \hat{f}(X)}{\partial X} & 1 \end{pmatrix} \right| = 1, \\ |\det(J_{Y \rightarrow X})| &= \left| \det \begin{pmatrix} \frac{\partial Y'}{\partial X} & \frac{\partial Y'}{\partial Y} \\ \frac{\partial \hat{N}_X}{\partial X} & \frac{\partial \hat{N}_X}{\partial Y} \end{pmatrix} \right| = \left| \det \begin{pmatrix} \frac{\partial Y}{\partial(X - \hat{g}(Y))} & \frac{\partial Y}{\partial(X - \hat{g}(Y))} \\ \frac{\partial Y}{\partial X} & \frac{\partial Y}{\partial Y} \end{pmatrix} \right| = \left| \det \begin{pmatrix} 0 & 1 \\ 1 & -\frac{\partial \hat{g}(Y)}{\partial Y} \end{pmatrix} \right| = 1, \end{aligned} \quad (\text{E.5})$$

where $J_{X \rightarrow Y}$ denotes the Jacobian matrix of the transformation from $(X, Y)^T$ to $(X', \hat{N}_Y)^T$ and $J_{Y \rightarrow X}$ vice versa.

Thus using Eq. (E.5), we rewrite the last terms in both sides of (E.3):

$$\begin{aligned} \mathbb{E} \log p(X, \hat{N}_Y) &= \mathbb{E} \log p(X', \hat{N}_Y) = \mathbb{E}(\log p(X, Y) / |\det(J_{X \rightarrow Y})|) = \mathbb{E} \log p(X, Y) \\ \mathbb{E} \log p(Y, \hat{N}_X) &= \mathbb{E} \log p(Y', \hat{N}_X) = \mathbb{E}(\log p(X, Y) / |\det(J_{Y \rightarrow X})|) = \mathbb{E} \log p(X, Y) \end{aligned} \quad (\text{E.6})$$

Using (E.3) and (E.6), we obtain:

$$H(X) + H(\hat{N}_Y) < H(Y) + H(\hat{N}_X), \quad (\text{E.7})$$

which finishes the proof. \square

Table 1: Parameter Settings

Parameter	Symbol	Value	Applicable to
threshold on W	ω	0.3	all
acyclity penalty	$h(W)$	$tr(e^{W \circ W}) - d$	NOTEARS, NOTEARS-MLP, ours, ours-MLP
acyclity penalty	$h(W)$	$tr\left(\left(I + \frac{W \circ W}{d}\right)^d\right) - d$	DAG-GNN
h tolerance	ϵ	10^{-8}	all
h progress rate	c	0.25	all
initial Lagrange multiplier	α_0	0	all
ρ increase factor		10	all
ρ maximum		10^{16}	all
optimize algorithms		L-BFGS	NOTEARS, NOTEARS-MLP, ours, ours-MLP
optimize algorithms		Adam	DAG-GNN
seed		123	all

F Additional Experimental Details

F.1 Algorithm Parameter Settings

Parameter settings for all algorithms are shown in Table 1. We use the least-squares loss $\frac{1}{2m} \|\mathbf{X} - \mathbf{X}W\|_F^2 + \lambda \|W\|_1$ regardless of the noise type for NOTEARS [Zheng et al., 2018] and NOTEARS-MLP [Zheng et al., 2020]. We use the negative ELBO as the object function under standard Gaussian noise assumption for DAG-GNN [Yu et al., 2019]. For **our** and **our-MLP**, we use entropy-based loss as the objective function. The NOTEARS code is available at <https://github.com/xunzheng/notears> and the DAG-GNN code is available at <https://github.com/fishmoon1234/DAG-GNN>. Our code is available at Supplemental Material.

F.2 Computing Environment

Solution times were obtained using a single CPU (Intel(R) Xeon(R) CPU E5-2620 v3 @ 2.40GHz).

F.3 License

We strictly follow the agreement of Apache-2.0 license used by NOTEARS code and do not use NOTEARS code commercially.